Journal of Applied Polymer Science

Structure and oxygen-barrier properties of (linear low-density polyethylene/ethylene–vinyl alcohol copolymer)/linear low-density polyethylene composite films prepared by microlayer coextrusion

Huijun Su, Juan Xue, Peiling Cai, Jiang Li, Shaoyun Guo

State Key Laboratory of Polymer Materials Engineering, Polymer Research Institute of Sichuan University, Chengdu 610065, China

Correspondence to: J. Li (E-mail: li_jiang@scu.edu.cn) and S. Guo (E-mail: nic7702@scu.edu.cn)

ABSTRACT: Ethylene–vinyl alcohol copolymer (EVOH) and linear low-density polyethylene (LLDPE) blends with 5% LLDPE grafted with 1% maleic anhydride (MAH; EVOH/LLDPE/LLDPE-*g*-MAH), created to increase the interfacial compatibility, were coextruded with pure LLDPE through the microlayer coextrusion technology. The phase morphology and gas-barrier properties of the alternating-layered (EVOH/LLDPE/LLDPE-*g*-MAH)/LLDPE composites were studied by scanning electron microscopy observation and oxygen permeation coefficient measurement. The experimental results show that the EVOH/LLDPE/LLDPE-*g*-MAH and LLDPE layers were parallel to each other, and the continuity of each layer was clearly evident. This structure greatly decreased the oxygen permeability coefficient compared to the pure LLDPE and the barrier percolation threshold because of the existence of the LLDPE/EVOH/LLDPE-*g*-MAH blend layers, and the LLDPE layers diluted the concentration of EVOH in the whole composites. In addition, the effects of the layer thickness ratio of the EVOH/LLDPE/LLDPE-*g*-MAH and LLDPE layers and the layer number on the barrier properties of the layered composites were investigated. © 2015 Wiley Periodicals, Inc. J. Appl. Polym. Sci. **2015**, *132*, 42211.

KEYWORDS: applications; films; oil and gas; property relations; structure

Received 3 December 2014; accepted 4 March 2015
DOI: 10.1002/app.42211

INTRODUCTION

For more than 40 years, polyolefins, such as polyethylene and polypropylene (PP), have been attracting major attention as packaging materials because of their outstanding light weight, flexibility, strength, transparency, and facile processability.[1,2] However, there is an inevitable intrinsic disadvantage, which is their high permeability to nonpolar gases (e.g., O_2, CO_2, etc.) everywhere; this has partially limited their practical applications. Although known to be highly sensitive to temperature and humidity, ethylene–vinyl alcohol copolymer (EVOH) has an excellent resistance to those nonpolar gases. Therefore, EVOH/polyolefin blends were developed as proposed packaging substitutes.[3] There was a barrier percolation composition threshold.[4–6] A significant decrease[7–9] in the permeation coefficient was observed above a rather narrow concentration range (≥15 wt %) of EVOH. Usually, conventional blending methods result in a high EVOH-barrier percolation threshold.[10] This result markedly increased the product cost because the price of EVOH is much higher than that of the polyolefins.[11] Moreover, many of the desirable properties, especially the mechanical properties of the polyolefins, were neither compromised nor lost with the high content of EVOH. Therefore, it is still a challenge to prepare low-cost [linear low-density polyethylene (LLDPE)/EVOH/LLDPE-*g*-maleic anhydride (MAH)]/LLDPE effective composites, with a low-barrier percolation threshold.

Commonly, there have been two methods for decreasing the concentrations of EVOH in composites. These include lamellar blending and traditional coextrusion. In a previous report, Yeo *et al.*[12] used the biaxial oriented film method to prepare PP/EVOH composites with a laminar structure of the EVOH. It exhibited improved barrier properties by 10 orders of magnitude. Yeh and coworkers[13,14] reported that high-density polyethylene (HDPE) composites containing 10 wt % modified polyamide (MPA) or MPA–EVOH in blown bottles with a laminar structure showed a higher oxygen barrier than pure HDPE at 40°C. However, the formation of stable two-dimensional sheets in polymer blends is closely related to several basic parameters, including the composition, viscosity ratio, interfacial tension, and processing conditions, which are hard to control in practical processing.[11] Another effective technology is traditional coextrusion, which can be used to prepare low-percolation-threshold and high-oxygen-barrier materials with a continuous layered structure.[13,14] Unfortunately, the composites prepared through this kind of method possess limited layer

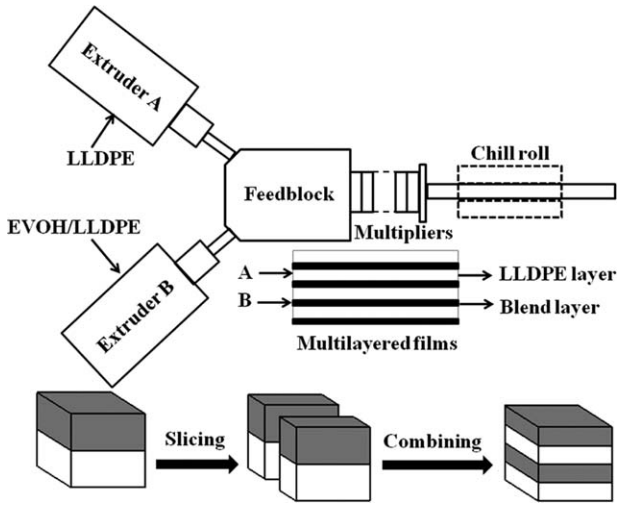

Figure 1. Schematic illustration of the multilayer coextrusion used to prepare the alternating $(AB)^n$ microlayered (EVOH/LLDPE/LLDPE-*g*-MAH)/LLDPE films.

numbers ($\leq$11) and higher cost because of the need for more extruders.

Recently, an original and improved microlayer coextrusion technology was developed to attain high gas-barrier properties.[15–17] For instance, Anne Hiltner's group[18,19] used this technology to obtain the high oxygen-barrier properties by subsequent biaxial drawing. The technology developed in our laboratory was also able to prepare composites with an alternating-layered structure from tens to thousands of layers with only two extruders, as shown in Figure 1. Through this technology, some properties of polymer materials were outstandingly improved because of their special double-continuous structure. For example, Xu *et al.*[20] in our group prepared electrically conducting composites with alternating layers of pure PP and carbon-black-filled PP, which showed a double percolation effect and a low-conducting percolation threshold and electrical resistivity. Lei *et al.*[21] in our group prepared HDPE/polyamide 6 (PA6) composite films with alternating HDPE and PA6 microlayers; these exhibited excellent gas-barrier properties. However, layered composites with two kinds of immiscible polymers not only led to a higher barrier percolation threshold (>24 wt % PA6), but they also have a weak interfacial adhesion, and this seriously limits their application. To solve these problems, the barrier layer in this study was designed to be a layered blend, in which one phase was the barrier material, and the other phase was the same polyolefin. Therefore, through this structural design, we further decreased the use of the barrier material and enhanced the interface strength. In this research, (EVOH/LLDPE/LLDPE-*g*-MAH)/LLDPE composites with alternating layers were prepared through microlayer coextrusion. The as-prepared composites exhibited an $(AB)^n$ (where n = 0,1,2,3...) alternating-layered structure, in which A and B were the LLDPE and EVOH/LLDPE/LLDPE-*g*-MAH blend layers, respectively. Compared to composites obtained by traditional blending methods, the EVOH/LLDPE composites prepared with microlayer coextrusion had a much lower EVOH concentration and much better oxygen-barrier properties. The outstanding oxygen-barrier properties were mainly attributed to the formation of the continuous EVOH phase in the blend layer. We suggest that the prepared (EVOH/LLDPE)/LLDPE composites should have applications in the packing industry because of their low-cost production and excellent oxygen-barrier properties.

EXPERIMENTAL

Materials

An extrusion-grade LLDPE (ELITE5220 G grade, density = 0.915 g/cm^3, melt flow index = 3.5 g/10 min, 190°C, 2.16 kg) was provided by Dow Chemical Co., Ltd. EVOH (DC3212HB grade, ethylene content = 32 mol %, density = 1.19 g/cm^3, melt flow index = 12 g/10 min, 210°C, 2.16 kg) was purchased from Nippon Synthetic Chemical Industry Co., Ltd. (Japan). LLDPE-*g*-MAH (MC216 grade, grafting degree = 1.0 wt %, melt flow index = 1.5 g/10 min, 190°C, 2.16 kg) was obtained from Ningbo Nengzhiguang New Materials Technology Co., Ltd. (China).

Preparation Through Conventional Melt Blending

Before melt blending, the EVOH and LLDPE-*g*-MAH were dried at 80°C for 12 h. EVOH/LLDPE/LLDPE-*g*-MAH composites with various weight ratios (10/85/5, 30/65/5, 40/55/5, 50/45/5, 60/35/5, 70/25/5, and 90/5/5) were prepared with a corotating twin-screw extruder (SHJ-20, Nanjing GIANT Machinery Co., Ltd., China) with a screw diameter of 20 mm and length-to-diameter ratio of 40/1. The extruder was operated at the following temperatures, T_1 = 100°C, T_2 = 200°C, T_3 = 210°C, and T_4 (die) = 200°C, along the extruder from the feed segment to the discharging segment with a screw speed of 20 rpm. The previous processing requirements were chosen to ensure the viscosity ratio of EVOH and LLDPE. The viscosity ratio was close to 1.0, as determined by the viscometer (Goettfrt Rheograph 2002 version 3.3.2, Germany). The blends obtained from the twin-screw extruder were quenched in cold water and were then cut into pellet particles for compression molding or microlayer coextrusion. For comparison, pure EVOH and pure LLDPE were also extruded under the same conditions.

Before compression molding, the EVOH/LLDPE/LLDPE-*g*-MAH blend pellets were dried at 80°C for 12 h. The compressed films of the blends about 0.8 mm in thickness were prepared by the following steps: pellet particles were placed between two Teflon plates, preheated without pressure for 10 min at 210°C, and then pressed at the same temperature under 12 MPa for 5 min. The obtained blends were cold-pressed in another press at room temperature for 5 min.

Preparation Through Microlayer Coextrusion

Figure 1 is a schematic illustration of the alternating-layered composite film preparation through microlayer coextrusion. Before preparation, EVOH/LLDPE pellets, including 5-phr LLDPE-*g*-MAH (compatilizer), which were prepared with the method discussed previously, were dried at 80°C for 12 h. The EVOH/LLDPE/LLDPE-*g*-MAH blend, as the B layer, was coextruded with LLDPE, as the A layer, by a microlayered coextrusion system designed in our laboratory. As the schematic of this system shows in Figure 1, alternating microlayered membranes about 0.8 mm thick and 50 mm wide were prepared. During

processing, the B and A layers were extruded from two extruders and combined as a two-layer melt in the feed block. They then flowed through a series of laminating–multiplying elements (LMEs). In one LME, the melt was sliced by a divider into two left and right sections 20 mm wide and then recombined vertically, as shown in Figure 1. An assembly of n LMEs could produce microlayered composites with $2^{(n+1)}$ layers. In this research, the coextrusion was performed with 0, 2, 3, 4, and 5 LMEs, which produced microlayered membranes with 2, 8, 16, 32 and 64 layers, respectively. The ratio of the thicknesses of the two component layers was varied by the adjustment of the screw speed of the extruders and precisely determined by extraction experiments. The temperatures of the two extruder dies for EVOH/LLDPE/LLDPE-*g*-MAH and LLDPE were 210 and 160°C, respectively, and the temperature of the LME was kept at 210°C. Because the viscosities of the B layer and the A layer were matched at 210°C for coextrusion, a continuous and regular layered structure was obtained (shown later in Figure 4).

Morphological Analysis

To observe the morphology of the blends prepared by compression molding and microlayer coextrusion, the two kinds of samples were fractured in liquid nitrogen. For the EVOH/LLDPE/LLDPE-*g*-MAH blend films prepared by compression molding, EVOH was etched with formic acid for 4 h when the EVOH content was less than 50 wt %; the LLDPE phase was etched with hot xylene for 4 h at 100°C when the EVOH concentration was equal to and greater than 50 wt %. For composite films prepared by microlayer coextrusion, the fractured sections were not etched. All of the fracture surfaces were sputtered with gold and then observed through scanning electron microscopy (SEM; FEI INSPECT F, Holland).

Oxygen-Barrier Measurements

The oxygen permeability coefficient (OPC) was measured with a pressure-difference gas permeation instrument (VAC-V1) produced by Labthink Instrument Co., Ltd. (China). The gas permeation instrument included an upper chamber, where the gas pressure was maintained at an atmospheric pressure, and a lower chamber, which was vacuumed before the tests. There was a room between the upper and lower chambers where the sample film was fixed. Before measurement, all of the samples were cut into circular membranes with a diameter of 50 mm and were then dried for 24 h at 85°C in an oven. The test temperature was kept at 40°C, and the test gas was oxygen. Through the gas permeability test, conducted in accordance with GB/T1038–2000, the curve of pressure in the lower chamber versus time of each sample was obtained. OPC was calculated according to the following calculation:

$$\mathrm{OPC}=\frac{\Delta P}{\Delta t}\times\frac{V}{S}\times\frac{T_0}{P_0T}\times\frac{D}{(P_1-P_2)}$$

where $\Delta P/\Delta t$ is the average value of the pressure change per unit time, V is the volume of the low-pressure chamber, S is the measured sample area, T is the testing temperature, T_0 is 273 K, P_0 is 1.01×10^5 Pa, D is the thickness of the sample, and the difference between pressures P_1 and P_2 is nearly equal to an atmospheric pressure.

EVOH Concentration Measurements

The compositions of the microlayered and conventional samples were measured by an extraction experiment. A certain amount of sample was weighed and subjected to Soxhlet extraction through the boiling of formic acid for 24 h. The residual undissolved substance was dried until its weight was constant. The EVOH content (EVOH wt %) was calculated with the following equation:

$$\mathrm{EVOH\ (wt\ \%)}=\frac{W_i-W_e}{W_i}\times100\%$$

where W_i is the weight of the sample before the extraction experiment and W_e is the weight of the dried, undissolved substance after the extraction experiment.

RESULTS AND DISCUSSION

Barrier Properties of the Conventional Blends

Theoretical models [eqs. (1) and (2)] were used to calculate the gas permeability of the composites prepared through conventional blending.[22] When the permeability coefficient of the continuous phase (P_a) is larger, eq. (1) should be used. Contrarily, eq. (2) is used when the permeability of the discontinuous phase is larger:

$$P=P_a\beta_a+P_b\beta_b \quad (1)$$

$$\frac{1}{P}=\frac{\beta_a}{P_a}+\frac{\beta_b}{P_b} \quad (2)$$

where β_a is the weight fraction of the continuous phase and β_b is the weight fraction of the disperse phase. Similarly, P_a and P_b are the gas permeability coefficients of the corresponding phases. P is the total gas permeability of the blend. From the SEM observations of the composites, as shown in Figure 2, when the EVOH content was less than 50 wt %, the continuous phase was LLDPE. Because the permeability coefficient of LLDPE was larger than that of EVOH, eq. (1) was used. When the EVOH concentration was equal to or greater than 50 wt %, the continuous phase was EVOH, and eq. (2) was used. The theoretical oxygen permeability coefficient (P_T's) as a function of the various EVOH concentrations in the composites prepared through compression molding; these values were calculated with eqs. (1) and (2) are shown in Figure 3 as a dashed line. The experimental oxygen permeability coefficient (P_E) values are also shown in Figure 3 as a solid line. It was very obvious that P_T and P_E were almost the same at every EVOH concentration. The theoretical and experimental curves both revealed the percolation phenomenon. When the content of EVOH was about 50 wt %, a significant decrease of two or three orders of magnitude of the permeability coefficient was observed. P_E decreased suddenly from 6.291×10^{-14} cm^3 cm cm^{-2}·s^{-1}·Pa^{-1} (40 wt %) to 2.3×10^{-16} cm^3 cm cm^{-2}·s^{-1}·Pa^{-1} (50 wt %), a reduction by a factor of 269.9. When the concentration of the EVOH was 70 wt % in the composites, P_E was 1.7×10^{-16} cm^3 cm cm^{-2}·s^{-1}·Pa^{-1}, a value similar to that of the pure EVOH. This indicated that the barrier percolation threshold for conventional LLDPE/EVOH composites was 50 wt %; this was a relatively high value compared to the weight fraction.

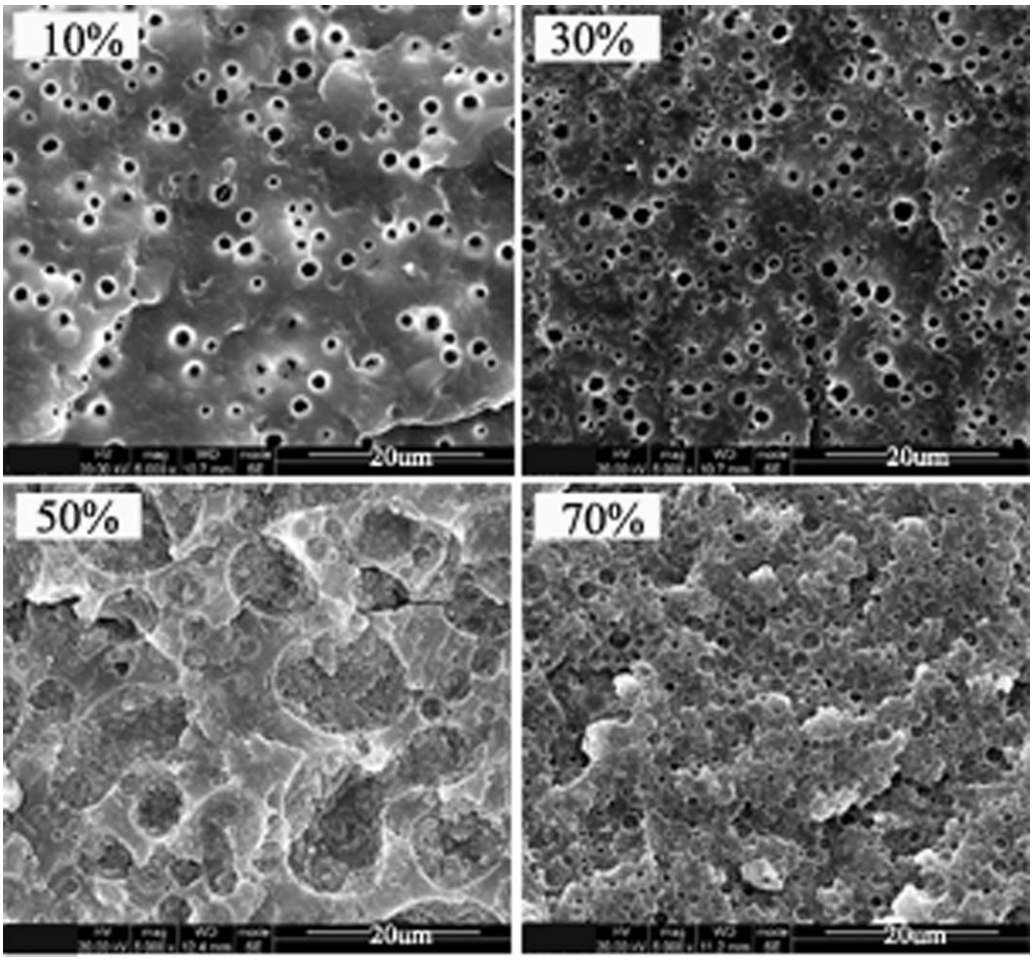

Figure 2. SEM images of the EVOH/LLDPE composites with various EVOH concentrations (10, 30, 50, and 70 wt %) prepared through compression molding and etched with formic acid.

Barrier Properties of the Microlayered Composites

OPC of 16-Layered Composites with Various EVOH Concentrations in the Blend Layer. The EVOH/LLDPE/LLDPE-*g*-MAH (10/85/5, 30/65/5, 40/55/5, 50/45/5, 60/35/5, 70/25/5, 90/5/5 w/w) composites (B) were obtained through melt blending with a twin-screw extruder and were coextruded with LLDPE (A) to form 16-layered alternating $(AB)^n$ composites. We controlled the ratio of the thickness of the A and B layers by controlling the rate of extruders of A and B at 1.5 : 1. Figure 4 shows the alternating $(AB)^n$ composites with 50 wt % EVOH in the B layer. The LLDPE and EVOH/LLDPE layers were parallel to each other, and the continuity of each layer was clearly evident.

Diffusion through this layered structure can be described by a series model. Schrenk and Alfrey[23] researched the relationship between the permeability coefficient of material and the series

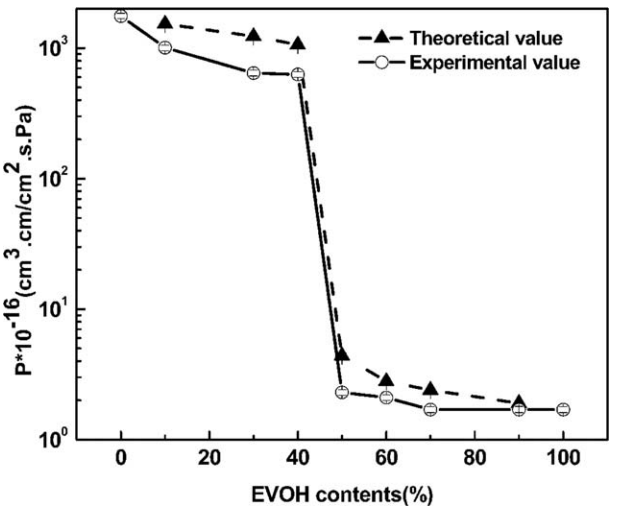

Figure 3. OPC of the EVOH/LLDPE composites with various EVOH concentrations prepared by compression molding.

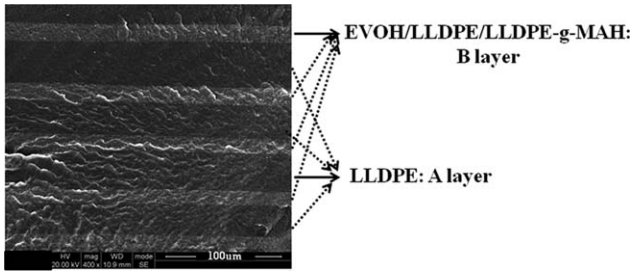

Figure 4. SEM image of part of a 16-layered alternating $(AB)^n$ composite with 50 wt % EVOH in the B layer.

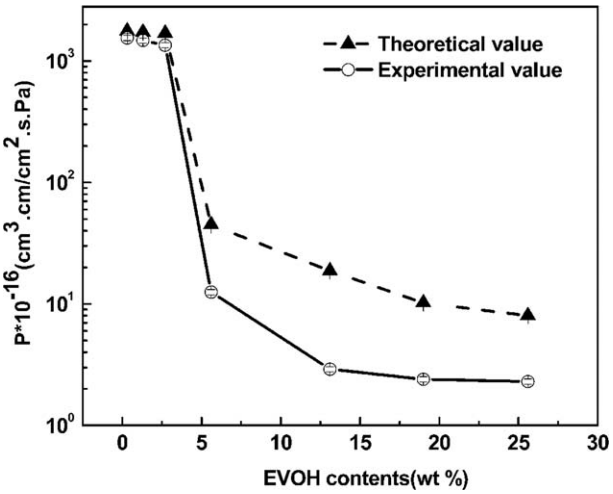

Figure 5. OPC of the microlayer composites with 16 layers and various EVOH concentrations in the whole film.

parallel structure and the permeability coefficient of each component, and its layer thickness of the resulting equation was as follows:

$$\frac{L}{P}=\frac{L_1}{P_1}+\frac{L_2}{P_2}+\frac{L_3}{P_3}\cdots+\frac{L_n}{P_n} \tag{3}$$

where L is the total thickness and L_n and P_n represent the thicknesses and permeability coefficients of the nth layer, respectively.

For our alternating-layered samples with $2n$ layers, the previous formula can be expressed as follows:

$$\frac{L}{P}=n\frac{L_{\mathrm{EVOH}}}{P_{\mathrm{EVOH}}}+n\frac{L_{\mathrm{PE}}}{P_{\mathrm{PE}}} \tag{4}$$

where L_{EVOH} is the thickness of the blend layer (B layer), L_{PE} is the thickness of the pure LLDPE layer (A layer), P_{EVOH} is the permeability coefficient of the blend layer, P_{PE} is the permeability coefficient of the pure LLDPE layer. When $nL_{\mathrm{EVOH}}/L=\phi_{\mathrm{EVOH}}$ and $nL_{\mathrm{PE}}/L=\phi_{\mathrm{PE}}$, where ϕ_{EVOH}, and ϕ_{PE} represent the volume contents of the EVOH/LLDPE/LLDPE-*g*-MAH blend layer and pure LLDPE layer, respectively, eq. (4) can be expressed as follows:

$$\frac{1}{P}=\frac{\phi_{\mathrm{EVOH}}}{P_{\mathrm{EVOH}}}+\frac{\phi_{\mathrm{PE}}}{P_{\mathrm{PE}}} \tag{5}$$

where ϕ_{EVOH} and ϕ_{PE} are the volume contents of the EVOH/LLDPE/LLDPE-*g*-MAH blend layer (B layer) and pure LLDPE layer (A layer), respectively. The theoretical OPC for the 16-layered composites was calculated according to eq. (6) and is shown in Figure 5:

$$\mathrm{OPC}=\frac{\phi_A}{P_A}+\frac{\phi_B}{P_B} \tag{6}$$

The experimental OPC curve of the 16-layered composites with various EVOH concentrations is also shown in Figure 5. The OPCs of the 16-layered microlayer composites with various EVOH concentrations in the blend layer decreased markedly from 1.3×10^{-13} to 1.3×10^{-15} cm^3 cm cm^{-2}·s^{-1}·Pa^{-1} as the EVOH concentration increased from 40 to 50 wt %. With the further increases in the concentrations of EVOH to 60 wt % and even 90 wt %, the OPC decreased from 2.9×10^{-16} cm^3 cm cm^{-2}·s^{-1}·Pa^{-1} to a smaller value. It was very obvious that the percolation threshold of both theoretical and experimental curves was about 5.6 wt % EVOH in the whole film. At the percolation point, the content of EVOH in the B layers was 50 wt %. As shown in Figure 6, the EVOH phase in B layers was still continuous when the content of EVOH in B layers was 50 wt %. Therefore, the continuous EVOH phase prevented the gas molecules from permeating into the materials. The existence of the LLDPE layer diluted the concentration of EVOH in the whole composite. This led to a large decrease in the percolation threshold.

Our previous work[24,25] revealed that the polymer melts underwent a strong shearing force when they flowed through the LME. As a result, the EVOH phase deformed and oriented along the flow direction; this was beneficial to the formation of a continuous EVOH phase and the improvement of the gas-barrier properties. Therefore, the experimental values of OPC were lower than the theoretical ones, as shown in Figure 5.

Effect of the Thickness of the B Layer on OPC.. To discuss the effect of the thickness of the B layer on OPC, we adjusted the ratio of thickness of the B and A layers by changing the rotation ratio of two extruders. In this section, the content of EVOH in the B layers for all of the samples was 50 wt %. Figure 7 shows that double-continuous phases of EVOH and LLDPE were formed in the B layers. However, changing the thickness of the B layer resulted in the content of EVOH in the whole material increasing linearly with the increasing ratio of the thickness of the B layers. Figure 8 shows the relationship of OPC and the ratio of layer thickness. With increasing layer thickness ratio from 0.02 to 0.08, the corresponding OPC decreased dramatically from 1.5×10^{-13} to 2.9×10^{-14} cm^3 cm cm^{-2}·s^{-1}·Pa^{-1}. This was attributed to the following reason: the thin B layer was easily broken when the layer thickness ratio of the B and A layers was very small. As a result, gas could easily permeate the sample through the breakage sites. With a further increase in the layer thickness ratio, the B layer became thick, and its continuity remained because the thick B layer was not easily broken. Therefore, when the thickness ratio of the B and A layers was larger than 0.08, the OPC of the materials was very small and tended to a limiting value.

Effects of the LMEs on the OPC of the Microlayer Composites. Previous research showed that the experimental OPC of the 16-layered samples was lower than the theoretical values (see Figure 5). The reason was that the double-continuous phase could be optimized, that is, the continuity of the EVOH phase improved when the melts flowed through the LMEs. Therefore, the layer number of the microlayer composites might have affected the OPC. Figure 9 indicates that the relationship between the OPC and the whole layer number. Here, the thickness ratio of the A and B layers of all of the samples was 1. The theoretical OPC calculated by eq. (6) was about 4.6×10^{-16} cm^3 cm cm^{-2}·s^{-1}·Pa^{-1}; this was independent of the number of LMEs. With the layer number increasing from 2 to 64, all of the experimental values were lower than the theoretical OPC; this confirmed that the shearing field in the LMEs improved the continuity of the EVOH phase in the EVOH/LLDPE/LLDPE-*g*-

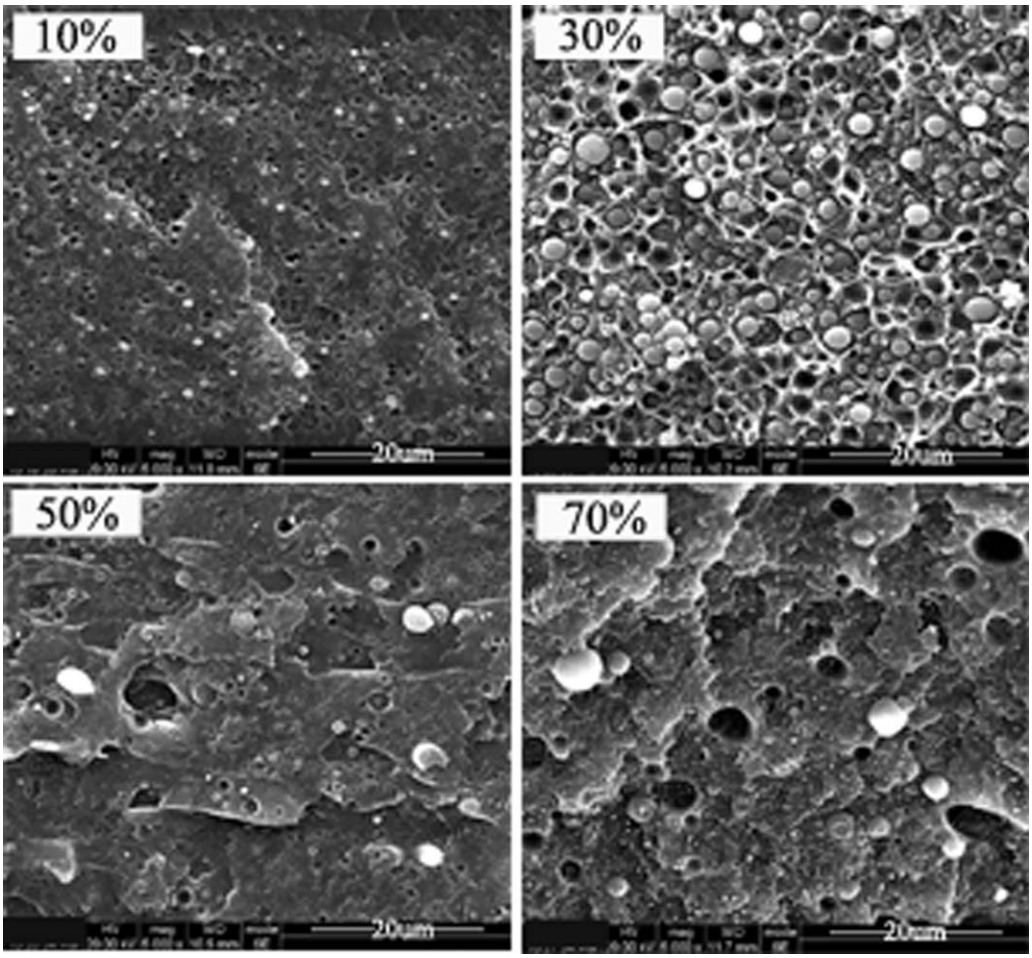

Figure 6. SEM images of the 16-layered microlayer composites with different EVOH concentrations in the blend layer.

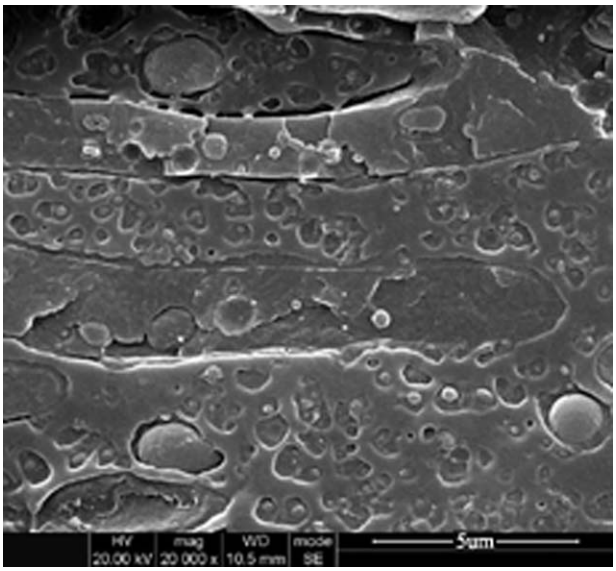

Figure 7. SEM image of the as-prepared microlayer composites with 16 layers and 50 wt % EVOH in the blend layer.

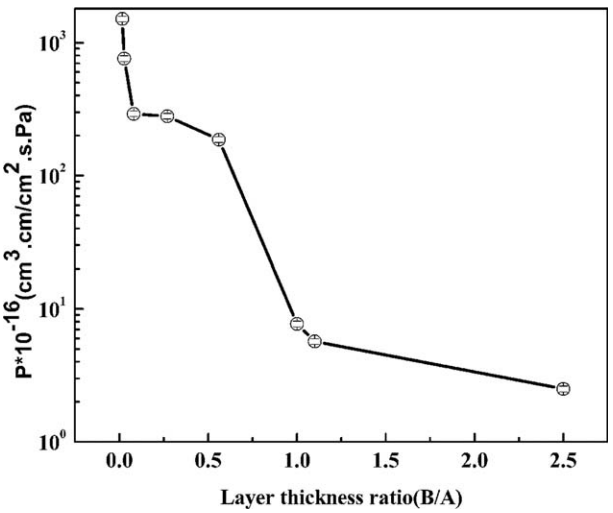

Figure 8. Effect of the ratio of the layer thickness on the OPC of the as-prepared microlayer composites with 16 layers and 50 wt % EVOH in the blend layer.

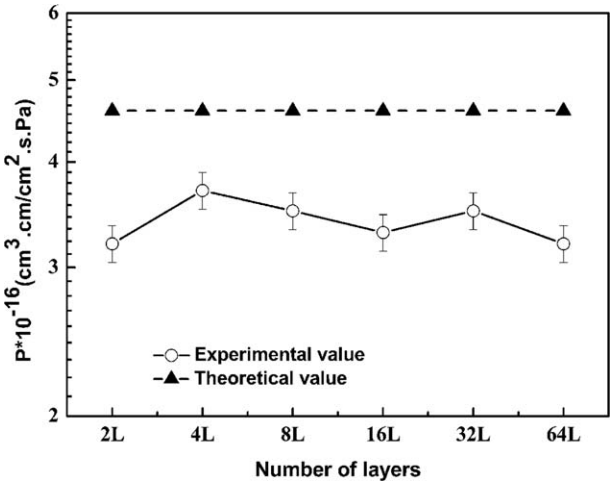

Figure 9. Effect of the layer number on the OPC of the microlayer composites with 50 wt % EVOH in the blend layer.

MAH blend layer. However, the layer number did not affect the experimental OPC, which fluctuated within a narrow range between 3.2×10^{-16} and 3.7×10^{-16} cm^3 cm $cm^{-2} \cdot s^{-1} \cdot Pa^{-1}$. This result reveals that more shearing action could not further increase the continuity of the EVOH phase in the blend layers.

CONCLUSIONS

Conventional EVOH/LLDPE/LLDPE-*g*-MAH blends and alternating-layered (EVOH/LLDPE/LLDPE-*g*-MAH)/LLDPE composites were prepared through compression molding and microlayer coextrusion, respectively. The gas-barrier percolation threshold of the conventional EVOH/LLDPE/LLDPE-*g*-MAH blends was about 50 wt % EVOH, at which the EVOH phase in the blend was continuous. For the alternating-layered (EVOH/LLDPE/LLDPE-*g*-MAH)/LLDPE composites with 16 layers, the gas-barrier percolation threshold decreased to about 5.6 wt % EVOH because the existence of the LLDPE layers diluted the concentration of EVOH in all of the composites. The thickness of the EVOH/LLDPE layer decided the quality of the barrier to the gas. When the layer thickness ratio of the EVOH/LLDPE and LLDPE layers changed from 0.02 to 0.08, the OPC of the 16-layered composite with 50 wt % EVOH in the blend layer was very high because the thin EVOH/LLDPE layer was easily broken. In addition, the experimental OPC of the layered sample was lower than theoretical value because the EVOH phase in the blend layer deformed and oriented along the flow direction; this was beneficial to the formation of the continuous EVOH phase and the improvement of the gas-barrier properties. However, an increase in the layer number did not decrease the OPC of the layered sample further.

ACKNOWLEDGMENTS

The authors are grateful to the National Natural Science Foundation of China (contract grant numbers 51227802, 50933004, 51073099, and 51121001), the Ministry of Education Priority Funding Areas (contract grant number 20110181130004), and the Program for New Century Excellent Talents in University (contract grant number NCET-10-0593) for their financial support of this work.

REFERENCES

1. Kim, S. W.; Chun, Y. H. *Korean J. Chem. Eng.* **1999**, *16*, 511.
2. Russo, P.; Acierno, D.; Di Maio, L. *Eur. Polym.* **1999**, *35*, 1261.
3. Smith, J. S.; Hui, Y. H. Industrial Oil and Fat Products, 5th ed., Wiley-Interscience: New York, **2005**; Chapter 5.
4. Lee, E. J.; Yoon, J. S.; Park, E. S. *Polym. Compos.* **2011**, *32*, 714.
5. Durmus, A.; Kasgoz, A.; Macosko, C. W. *Polymer* **2007**, *48*, 4492.
6. Marta, M. S.; Amparo, L. R.; Jose, M. L. *Biomacromolecules* **2012**, *13*, 3887.
7. Kamal, M. R.; Garmabi, H.; Hozhabr, S. *Polym. Eng. Sci.* **1995**, *35*, 41.
8. Walling, N.; Kamal, M. R. *Adv. Polym. Technol.* **1996**, *5*, 268.
9. Lee, S. Y.; Kim, S. C. *Polym. Eng. Sci.* **1997**, *37*, 463.
10. Harrats, C.; Thomas, S.; Groeninckx, G. Taylor & Francis: Boca Raton, FL, **2005**; Chapter 3.
11. Guilbert, S.; Guillaume, C.; Gontard, N. Springer: New York, **2011**; Chapter 26.
12. Yeo, J. H.; Lee, C. H.; Park, C. S.; Lee, K. J.; Nam, J. D.; Kim, S. W. *Adv. Polym. Technol.* **2001**, *20*, 191.
13. Yeh, J. T.; Huang, S. S.; Yao, W. H. *Macromol. Mater. Eng.* **2002**, *287*, 532.
14. Yeh, J. T.; Huang, S. S.; Yao, W. H.; Wang, I. J.; Chen, C. C. *J. Appl. Polym. Sci.* **2004**, *92*, 2528.
15. Garmabi, H.; Kamal, M. R. *Plast. Film Sheeting* **1999**, *15*, 120.
16. Guo, S. Y.; Wang, M.; Li, J.; Shen, J. B.; Xu, S. X; Du, Q. Chin. Pat. CN200970885 **2007**.
17. Guo, S. Y.; Wang, M.; Li, J.; Shen, J. B.; Xu, S. X; Du, Q. Chin. Pat. ZL200620036431.4 **2007**.
18. Gupta, M.; Lin, Y. J.; Deans, T.; Baer, E.; Hiltner, A.; Schiraldi, D. A. *Macromolecules* **2010**, *43*, 4230.
19. Carr, J. M.; Mackey, M.; Flandin, L.; Hiltner, A.; Baer, E. *Polymer* **2013**, *54*, 1679.
20. Xu, S. X.; Wen, M.; Li, J.; Guo, S. Y.; Wang, M.; Du, Q.; Shen, J. B.; Zhang, Y. Q.; Jiang, S. L. *Polymer* **2008**, *49*, 4861.
21. Lei, F.; Du, Q.; Li, T.; Li, J.; Guo, S. Y. *Polym. Eng. Sci.* **2013**, *53*, 1996.
22. Zhang, L. C.; Qu, X. W.; Ding, H. L. Polymer Science Chemical Industry: Beijing, **2007**; Chapter 2.
23. Alfrey, T., Jr.; Schrenk, W. *J. Science* **1980**, *208*, 813.
24. Shen, J. B.; Wang, M.; Li, J.; Guo, S. Y.; Xu, S. X.; Zhang, Y. Q.; Li, T.; Wen, M. *Eur. Polym. J.* **2009**, *45*, 3269.
25. Du, Q.; Jiang, G. J.; Li, J.; Guo, S. Y. *Polym. Eng. Sci.* **2010**, *50*, 1111.